

RSC Advances



This is an *Accepted Manuscript*, which has been through the Royal Society of Chemistry peer review process and has been accepted for publication.

Accepted Manuscripts are published online shortly after acceptance, before technical editing, formatting and proof reading. Using this free service, authors can make their results available to the community, in citable form, before we publish the edited article. This *Accepted Manuscript* will be replaced by the edited, formatted and paginated article as soon as this is available.

You can find more information about *Accepted Manuscripts* in the [Information for Authors](#).

Please note that technical editing may introduce minor changes to the text and/or graphics, which may alter content. The journal's standard [Terms & Conditions](#) and the [Ethical guidelines](#) still apply. In no event shall the Royal Society of Chemistry be held responsible for any errors or omissions in this *Accepted Manuscript* or any consequences arising from the use of any information it contains.

ARTICLE

Magnesium carbonate basic coating on cotton cloth as a novel adsorbent for removal uranium

Cite this: DOI: 10.1039/x0xx00000x

Lei Zhang,^a Xiaoyan Jing,^a Rumin Li,^a Qi Liu,^{*a} Jingyuan Liu,^a Hongsen Zhang,^a Songxia Hu^a and Jun Wang^{*ab}

Received 00th January 2012,
Accepted 00th January 2012

DOI: 10.1039/x0xx00000x

www.rsc.org/

The magnesium carbonate basic coating on the cotton cloth ($\text{Mg}_2\text{CO}_3(\text{OH})_2/\text{CC}$) was prepared by a facile and cost-effective method for uranium(VI) adsorption. The process of the obtained material for uranium(VI) adsorption on aqueous solution was fully researched. The results reveal that the maximum adsorption capacity of the $\text{Mg}_2\text{CO}_3(\text{OH})_2/\text{CC}$ toward uranium is 370mg/g, providing a strong efficiency for removal of uranium from aqueous solution. The experimental data were analyzed using adsorption kinetic models. The adsorption kinetics of uranium onto $\text{Mg}_2\text{CO}_3(\text{OH})_2/\text{CC}$ obey the pseudo-second-order model, indicating that the determining step might be chemical adsorption. The calculated thermodynamic parameters, such as ΔH° , ΔS° and ΔG° show that the adsorption process is spontaneous and endothermic. Furthermore, the as-prepared material can be easily separated from aqueous solution after adsorption. Such excellent performance may promote the promising and effective adsorbent for practical uranium(VI) adsorption.

1. Introduction

As a kind of nuclear fuel, uranium was widely used for military and civilian application.¹⁻⁵ However, uranium nuclear pretreatment usually causes serious environmental problems. Moreover, the limited underground uranium reserves could not match the urgent industry need.^{3,4} To address these problems, efforts have been paid to extracting uranium from unconventional sources such as industrial waste water and sea water containing rich-U.⁵

In comparison with other alternative methods,⁶ adsorption has raised significant concerns for several advantages, such as the relative freedom design of adsorbent, the insensitivity to toxic substances and the low operating costs.⁷ Additionally, it could avoid using toxic solvents and facilities to resource regeneration.⁸

The adsorption material for selective removal of uranium should also possess extreme thermostability and radioresistance due to the strong radioactivity and high temperature of the contained uranium in industrial waste water. Therefore, organic resins could not be used in the treatment of high radioactivity waste water for their low fusion point.⁹ The reported chelating resin (PS-PAMAM-PPA) has a long graft chain for adsorption of uranium.¹⁰ The prepared silica modified by the (3-mercaptopropyl)-trimethoxysilane was used for application in nuclear environmental remediation.¹¹ However, the grafting long chain and the modified functional groups were easily broken down under strong radiation and high temperature.

Thus, attention needs to shift more towards inorganic materials for their excellent radiation and thermal stability.¹²⁻¹⁴ Recently A. Hobaib et al. reported the use of BaTiO_3 for removal of uranyl ions from aqueous solutions.¹⁵ Singh prepared phosphate and goethite as sorbents for uptake of uranyl ions.¹⁶ They noted that the high adsorption capacity of barium titanate and phosphate is due to large surface area and porous structure. However, the inorganic powder adsorbents are uneasy to recover after use.¹⁷

As a proof-of-concept, we present a facile and cost-effective method to prepare a magnesium carbonate basic-based adsorbent for uranium adsorption from aqueous solution. As shown in Sch. 1, the synthesis process was divided into two parts: the modification of cotton cloth with EDTA and the interfacial assembly process of the magnesium carbonate basic on cotton cloth by hydrothermal. As an environmentally friendly



Sch. 1 Schematic diagram of preparation and adsorption.

-y and nontoxic material, $Mg_2CO_3(OH)_2$ possesses higher adsorption capacity of uranium than many other reported adsorbents and exhibits faster rate of adsorption.¹⁸⁻²⁰ Furthermore, a novel strategy to enables the enrichment and desorption of uranium and the recycling of $Mg_2CO_3(OH)_2$ simultaneously was also provided. Such excellent performance may promote the promising and effective adsorbent for practical uranium(VI) adsorption.

2. Experiment section

2.1. Reagents and chemicals

All chemicals were of reagent grade and all solutions were prepared in deionized water. Cotton cloth (medical) was obtained from local market. Uranyl nitrate $UO_2(NO_3)_2 \cdot 6H_2O$ was acquired from Aladdin Reagent Limited. Stock solution of uranium (VI) (1000 mg/L) was prepared by dissolving $UO_2(NO_3)_2 \cdot 6H_2O$ into deionized water. $Mg(NO_3)_2 \cdot 6H_2O$, $(NH_2)_2CO$ and H_2O_2 etc. were purchased from Tianjin Kermel Chemical Reagents Limited of China and used without further purification.

2.2. Material synthesis

Preparation of carboxylated cotton cloth: EDTAD was synthesized by the following method described by Osvaldo et al.^{21,22} To obtain modified cotton cloth, 1 g of cotton cloth was reacted with 3 g of EDTAD in 80mL anhydrous DMF for 24 h at 65 °C under continuous stirring. After filtration, the carboxylated cotton cloth was washed with DMF, deionized water, saturated sodium bicarbonate solution, deionized water, anhydrous ethanol, acetone, respectively, and then dried in an oven at 75 °C for 2 h, cooled down naturally to room temperature.

Preparation of the $Mg_2CO_3(OH)_2/CC$: Magnesium nitrate (3.8g) and urea (1.8g) were dissolved in deionized water (75mL). After stirring for 20 min, the mixed solution and 1g of carboxylated cotton cloth were then transferred into a Teflon-lined autoclave with a 75% filling ratio, and the autoclave was sealed and heated for 12 h at 100 °C, then left to cool in an oven. The resulting cotton cloth were washed with deionized water and anhydrous ethanol until neutral and then dried in a vacuum oven for 1 h at 50 °C.

2.3. Adsorption experiments

The adsorption of uranium (VI) was used as the following procedure: 0.01g of the $Mg_2CO_3(OH)_2/CC$ was equilibrated with 20 mL of uranium(VI) solution from the diluted stock solution at different initial concentrations, different temperature and different initial pH (adjusted with 0.5mol/L HNO_3 and 0.5mol/L $NaOH$) in a conical flask, then the conical flask was sealed and performed in a reciprocating water bath shaker with concussion speed of 150 rpm. At the end of the adsorption, the adsorbent containing uranium was removed with tweezers, then the equilibrium concentration of U (VI) in supernatant was

determined. Uranium adsorption capacity q_e (mg U g^{-1} dry adsorbent) were obtained by-using the following equations²³:

$$q_e = \frac{(C_0 - C_e)V}{m} \quad (1)$$

Where q_e is the adsorption capacity of adsorbent (mg/g) C_0 is the initial concentration of uranium (VI) (mg/L), C_e is the equilibrium concentration of uranium(VI) (mg/L), V is the volume of the testing solution, and m is the weight of the adsorbent.

2.4. Characterization

The XRD data of samples were collected on a Rigaku D/max-III B X-ray diffractometer with $Cu K\alpha$ irradiation operated at 40kV and 150mA. The scanning step was 0.02° in 2θ range of 10-80°. Surface morphology of samples was characterized on Philips XL30 scanning electron microscopy (SEM) coupled with an energy-dispersive X-ray spectrum (EDS). The FT-IR spectra was recorded on a AVATAR 360 Fourier transform infrared spectrometer. The uranium concentration was determined by WGJ-III Trace Uranium Analyzer from the Company of Hangzhou Daji Photoelectric Instrument.

3. Results and discussions

3.1. Characterization of samples

To coating with the magnesium carbonate basic, the cotton cloth was chemically modified by the esterification reaction with EDTAD.²⁴ The FT-IR spectra of cotton cloth and carboxylated cotton cloth confirm the chemical modification process (Fig. 1). The new strong band at 1741cm^{-1} for carboxylated cotton cloth could be attributed to stretching vibration due to presence of the ester group.²⁵ Moreover, the existence of strong bands at 1630cm^{-1} , 1596cm^{-1} and 1409cm^{-1} for carboxylated cotton cloth, which could indexed to stretching vibration of the carboxylate ion, was not seen in original cotton cloth.²⁶ Therefore, the FT-IR spectra analysis can prove the

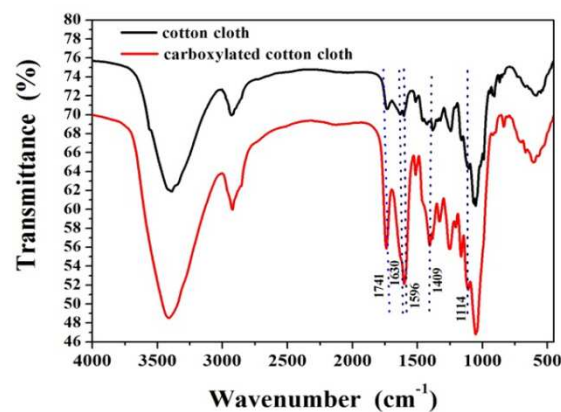


Fig. 1 The FTIR spectrum of cotton cloth and carboxylated cotton cloth.

successful introduction of the -COOH into cotton cloth. The chemical modification could highly facilitate the interfacial assembly process of the magnesium carbonate basic on cotton cloth. As shown on Fig. 2 a and b, the magnesium carbonate basic was successfully coated onto the carboxylate cotton cloth after chemical modification.

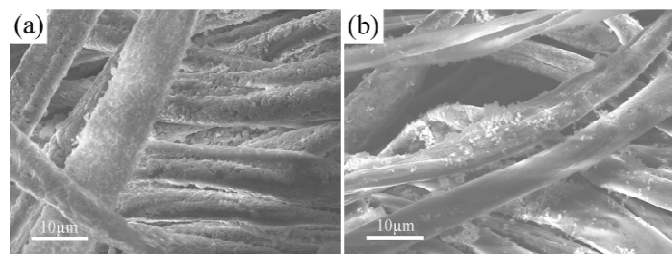


Fig. 2 (a) SEM image of as-prepared $\text{Mg}_2\text{CO}_3(\text{OH})_2/\text{CC}$ using the carboxylated cotton cloth; (b) SEM image of as-prepared $\text{Mg}_2\text{CO}_3(\text{OH})_2/\text{CC}$ using the non-carboxylated cotton cloth.

The interfacial assembly process of the magnesium carbonate basic on cotton cloth was performed by the hydrothermal

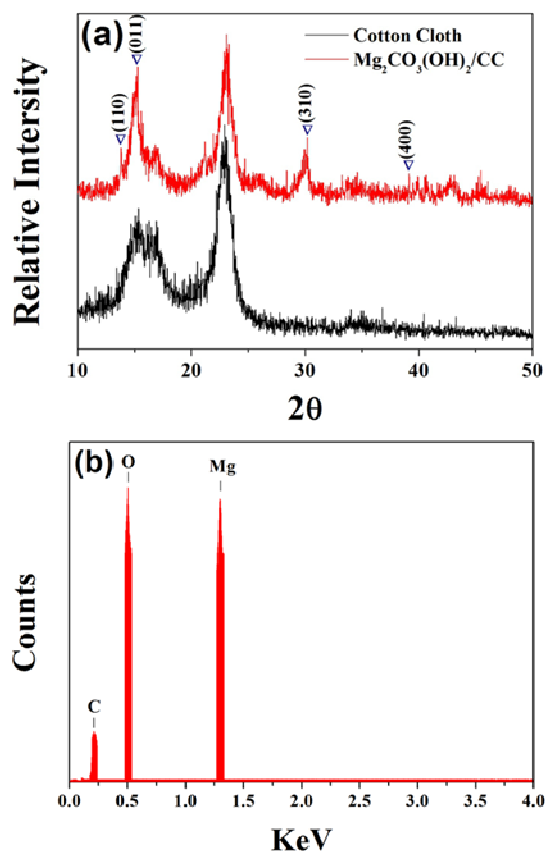


Fig. 3 (a) A typical XRD pattern of cotton cloth and $\text{Mg}_2\text{CO}_3(\text{OH})_2/\text{CC}$; (b) EDS analysis of $\text{Mg}_2\text{CO}_3(\text{OH})_2/\text{CC}$.

method.²⁷ Fig. 3a shows the XRD pattern of the original cotton cloth and the as-prepared $\text{Mg}_2\text{CO}_3(\text{OH})_2/\text{CC}$. The diffraction

pattern of the peaks for the as-prepared material at 2θ values of $13.8^\circ(110)$, $15.3^\circ(011)$, $30.8^\circ(310)$, $39.2^\circ(400)$ in the image, which are basically consistent with standard card (JCPDS No.25-0513). Therefore, it is able to deduce that the crystal structures of substance wrapped in cotton cloth are magnesium carbonate basic.²⁸ The Mg, C and O signals in the EDS analysis could further confirm that magnesium carbonate basic was coated on the surface of cotton cloth in the hydrothermal process (Fig. 3b).

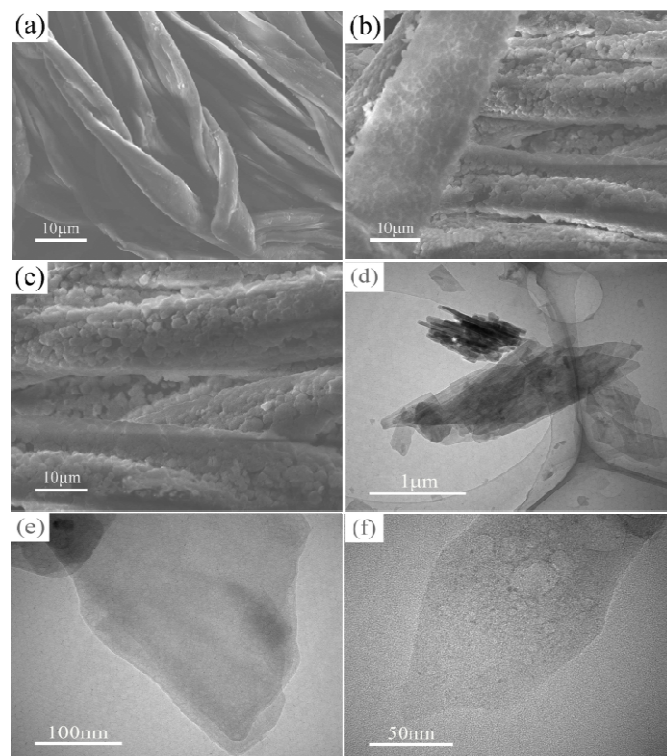


Fig. 4 (a) (b) (c) SEM images of the unprocessed cotton cloth, $\text{Mg}_2\text{CO}_3(\text{OH})_2/\text{CC}$ and sonicated $\text{Mg}_2\text{CO}_3(\text{OH})_2/\text{CC}$, respectively. (d) (e) and (f) TEM images at different magnifications of the $\text{Mg}_2\text{CO}_3(\text{OH})_2$.

SEM images of the untreated cotton cloth and the $\text{Mg}_2\text{CO}_3(\text{OH})_2$ coating on cotton cloth are shown in Fig. 4a and b, respectively. From Fig. 4b, it is clearly observed that the spherical particles of magnesium carbonate basic were closely attached on a cotton fiber. The seed crystal was formed with electrostatic attraction, hydrogen bonding and Van der Waals. Moreover, the free carboxyl groups were combined chemically. As a result, the crystals of magnesium carbonate basic were adsorbed on cotton fiber from aqueous solution. To demonstrate the attach strength of magnesium carbonate basic on the cotton cloth, the as-prepared material was sonicated for an 20min. As can be seen from Fig. 4c, the magnesium carbonate basic particles were not peeled off from the cotton fiber by ultrasound.

The microstructure of as-prepared magnesium carbonate basic was also further analyzed by TEM. Fig. 4d, e and f were clearly shown the magnesium carbonate basic coating on cotton fibers possess lamellar structure with hierarchically pores. The formation of pores with the estimated size of 6-8 nm may be

due to large amounts of carbon dioxide and water vapor which were generated during the calcification process of mixed solution. Nitrogen adsorption/desorption isotherm of as-prepared $\text{Mg}_2\text{CO}_3(\text{OH})_2$ was shown on Fig. S1. The curve was categorized as typical IV isotherms with a distinct hysteresis loop which is observed in the pressure range of 0.5-1.0 p/p_0 , demonstrating the existence of mesopore in the as-prepared material. The mesoporous feature of $\text{Mg}_2\text{CO}_3(\text{OH})_2$ could further confirmed by the pore-size distribution analysis, indicating a pore size arrange of 6-7 nm which is also consistent with the TEM analysis. The specific surface area was calculated to be about $128.20\text{m}^2/\text{g}$ which is highly facilities to the adsorption of uranium.

3.2. Effect of initial pH values

The pH of solution that affect both the speciation of uranium (VI) and surface state of adsorbent is one of the most important parameters for adsorption of uranyl ion.²⁹ The adsorption of uranium on $\text{Mg}_2\text{CO}_3(\text{OH})_2/\text{CC}$ was carried out at pH value ranging from 2.0 to 10.0 using 200 mg/L initial concentration of uranium solution at 298 K. Clearly, the adsorption capacity increased with the increase of pH, then reached the maximum at pH 5.0 and finally declined subsequently (Fig. 5). The presence of various compounds of uranium (VI) could be explained by hydrolysis of the from $[(\text{UO}_2)_p(\text{OH})_q]^{(2p-q)+}$ at different pH values. At low pH, the low adsorption capacity may be attributed to the competition of H^+ ions with uranyl ions on the adsorption sites of $\text{Mg}_2\text{CO}_3(\text{OH})_2/\text{CC}$. However, in the range from acidic to alkaline, the main hydroxide products of uranium(VI), such as $[\text{UO}_2(\text{OH})]^+$, $[(\text{UO}_2)_2(\text{OH})_2]^{2+}$ and $[(\text{UO}_2)_3(\text{OH})_5]^+$ were appeared in the solution and the UO_2^{2+} could not be combined with CO_3^{2-} of magnesium carbonate basic. Thus, the adsorption capacity was decreased.³⁰⁻³⁴ According to the above results, the best of pH value is 5.0.

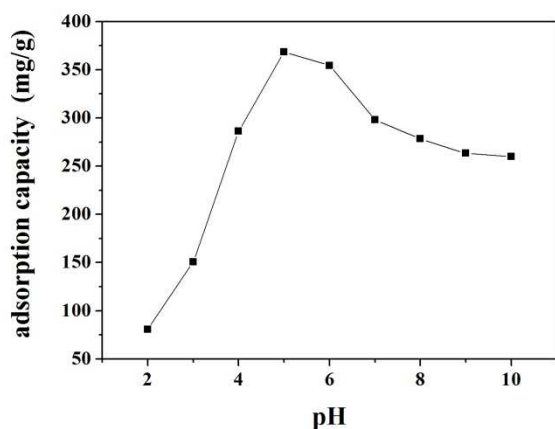


Fig. 5 Effect of pH on the adsorption of uranyl ions, $C_0=200\text{mg/L}$, $t=2\text{h}$, $T=298\text{K}$.

3.3. Effect of initial uranium(VI) concentration

For adsorption, the initial concentration is an important driving force to overcome transfer resistance of the uranyl ions in

aqueous solution.³⁵ Therefore, research was performed with initial uranium (VI) concentration ranged from 20 to 220 mg/L at 298K, 308K and 318K, respectively. As shown on the Fig. 6, three curves was displayed the increase of adsorption capacity with the initial increase in uranium (VI) concentration. It is clearly to observed that the more active sites of $\text{Mg}_2\text{CO}_3(\text{OH})_2/\text{CC}$ involved and the higher driving force which overcomes mass transfer resistance between solid and liquid obtained in the adsorption process, leading the increase of uranium in solution.³⁶ It also could be observed that the adsorption capacity gets up to a maximum (371.26mg/g) at the

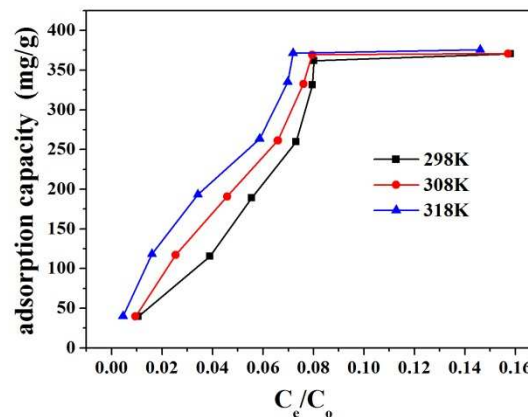


Fig.6 Isotherms of uranyl ions adsorption onto $\text{Mg}_2\text{CO}_3(\text{OH})_2/\text{CC}$, $\text{pH}=5$, $t=2\text{h}$.

uranium (VI) concentration of 200 mg/L and the adsorption capacity was enhanced with the increase of temperature. This phenomenon could be explained by the fact that adsorption sites have reached saturation and adsorption process is endothermic in nature. It also suggests that the $\text{Mg}_2\text{CO}_3(\text{OH})_2/\text{CC}$ exhibits excellent adsorption capacity, which is attributed to the strong binding ability between the uranyl ions and carbonate ions.

3.4. Adsorption isotherm

Adsorption equilibrium isotherm represents the mathematical relation of adsorption capacity (q_e (mg/g)) to the equilibrium solution concentration (C_e (mg/L)) at fixed temperature. The adsorption data was subjected to the Langmuir and Freundlich isotherms. As a theoretical model, the Langmuir isotherm has maximum adsorption capacity which was based on monolayer coverage of the adsorb in the surface of adsorbent.³⁷ The linear equation of can be expressed as the following equation:

$$\frac{C_e}{q_e} = \frac{1}{q_m K_L} + \frac{C_e}{q_m} \quad (2)$$

where K_L is the equilibrium constant (L/mg), q_m is the saturated monolayer adsorption capacity (mg/g). The linear plots of C_e/q_e versus C_e gives a value for q_m and K_L . As an empirical model, the Freundlich isotherm was also widely used. This model

assumes that several adsorption energies are involved at different sites.³⁸ The Freundlich isotherm can be represented by the following equation:

$$\ln q_e = \ln K_F + \frac{1}{n} \ln C_e \quad (3)$$

where n and $K_F[(\text{mg/g})(\text{L/mg})]^{1/n}$ are the intensity of sorption and the Freundlich constant that is related to adsorption capacity of the adsorbent, respectively. The linear plots of Langmuir and Freundlich equations for uranium (VI) adsorption are shown on Fig. 7. The relative parameters of the isotherm models were calculated and presented in Tab. S2. Comparing the values of R^2 which was obtained by the two

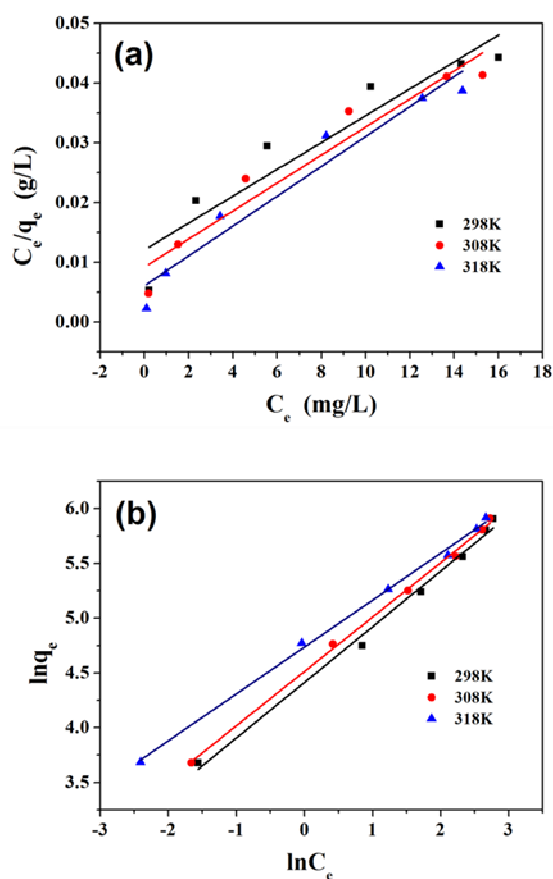


Fig. 7 (a) Langmuir adsorption isotherm; (b) Freundlich adsorption isotherm, at different temperatures, $C_0=200\text{mg/L}$, $\text{pH}=5$, $t=2\text{h}$.

isotherm models, it is confirm that the adsorption experimental data was better match with Freundlich model. The isotherm model has a multilayer adsorption on surface, which cannot predict any saturation of the adsorbent by the sorbate. The $1/n$ is generally between 0 and 1, the value of $1/n$ indicates the effect of concentration to the strength of adsorption. If the $1/n$ ranged 0.1 to 0.5, the adsorption is easily; However, when $1/n > 2$, the adsorption is difficult to occur.^{39, 40} The results show that the value of $1/n$ is between 0.1 and 0.5, so the uranyl ions

were easily combined with carbonate ions of $\text{Mg}_2\text{CO}_3(\text{OH})_2/\text{CC}$. The K_F shows the information about the bonding energy. The K_F increases with the rise of temperatures, revealing that the adsorption capacity of uranium (VI) on $\text{Mg}_2\text{CO}_3(\text{OH})_2/\text{CC}$ increases with the rise of temperature. It indicates that the present adsorption process on $\text{Mg}_2\text{CO}_3(\text{OH})_2/\text{CC}$ was probably dominated by a multilayer adsorption.

3.5. Thermodynamic study

The effect of temperature on the adsorption capacity of $\text{Mg}_2\text{CO}_3(\text{OH})_2/\text{CC}$ was also investigated. To evaluate the thermodynamic feasibility and understand the nature of the adsorption process,^{41, 42} the thermodynamic parameters such as standard free energy (ΔG°), standard enthalpy (ΔH°) and standard entropy (ΔS°) were calculated by the equations (4), (5) and (6).

$$\ln \frac{1}{C_e} = \ln K_F - \frac{\Delta H^\circ}{RT} \quad (4)$$

$$\Delta G^\circ = -nRT \quad (5)$$

$$\Delta S^\circ = \frac{\Delta H^\circ - \Delta G^\circ}{T} \quad (6)$$

where C_e (mg/L) is the equilibrium concentration, n is the fitting constant of Freundlich exponent, R is the gas constant ($8.314 \text{ J/mol} \cdot \text{K}$), K_F is the empirical constant of Freundlich and T (K) is temperature. The change of enthalpy was determined by the slope of the plots of $1/C_e$ versus $1/T$ (Fig. 8).

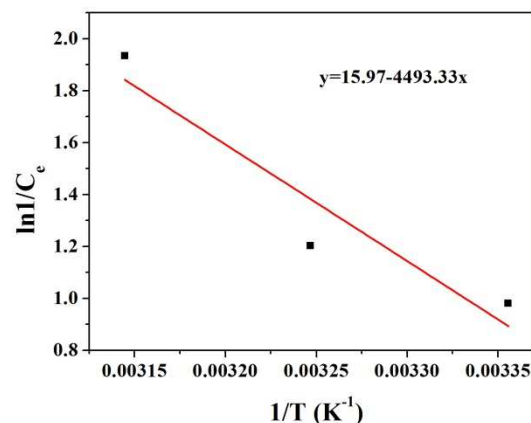


Fig. 8 Enthalpy determination curves for the adsorption of uranium on $\text{Mg}_2\text{CO}_3(\text{OH})_2/\text{CC}$, $q_e=50\text{mg/g}$, $\text{pH}=5$, $t=2\text{h}$.

According to Tab.S3, the negative values of ΔG° indicate the adsorption process is feasible and spontaneous. The numerical value of ΔG° decreases with the increase of temperature, revealing that high temperature is more favorable for the adsorption of uranium. The positive value of ΔH° indicates that

the adsorption process is endothermic. Since the adsorption is endothermic, the equilibrium adsorption capacity increases with the increase of temperature. The positive values of ΔS° reveal that the removal of uranyl ions on $\text{Mg}_2\text{CO}_3(\text{OH})_2/\text{CC}$ is stable.

3.6. Effect of contact time and adsorption dynamics

From Fig. 9, the adsorption amount of uranium (VI) increases with the increase of contact time and then gradually tends to keep unchanged at 50 min. The time taken to reach equilibrium

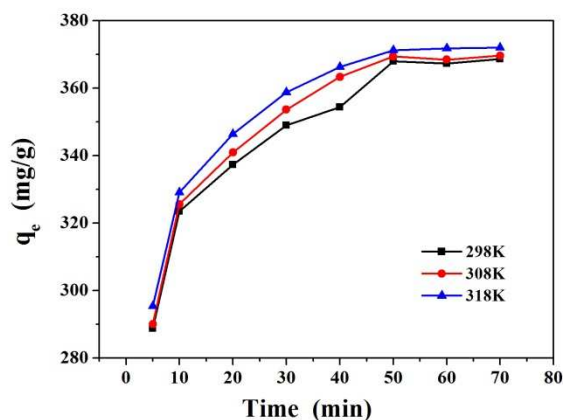


Fig. 9 Effect of contact time on the adsorption of uranium(VI), $C_0=200\text{mg/L}$, $\text{pH}=5$.

decreases and the equilibrium adsorption capacity increases with the increase of temperature. The initial sharp burst adsorption may be caused by the uranyl ions which were rapid adsorbed on exterior surfaces of adsorbent. When the adsorption reaches a saturation at the exterior surfaces, the resistance of uranyl ions which penetrate into the inner surfaces increases.⁴³⁻⁴⁵ After 1 h, the change of adsorption capacities for uranium (VI) does not show any notable effects.

To study the kinetic mechanism of the adsorption process, pseudo-first-order and pseudo-second-order models were used.⁴⁶⁻⁴⁸ The pseudo-first-order kinetic model is given as:

$$\ln(q_e - q_t) = \ln q_e - k_1 t \quad (7)$$

where k_1 (1/min) is the rate constant of pseudo-first-order adsorption, q_e (mg/g) and q_t (mg/g) are the amount of uranium adsorbed at equilibrium and time (t), respectively. The values of k_1 and q_e calculated from the Eq.(8), which are presented in Tab. S4. The low-related coefficient and the large differences between experimental and calculated values suggest that the pseudo-first-order kinetics model does not fit well with the experimental data. The plots of $\ln(q_e - q_t)$ versus t at different temperature in Fig. 10 (a). The pseudo-second-order kinetic model is defined as:

$$\frac{t}{q_t} = \frac{1}{k_2 q_e^2} + \frac{t}{q_e} \quad (8)$$

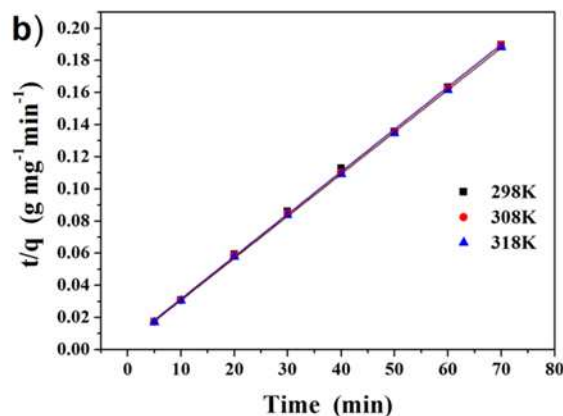
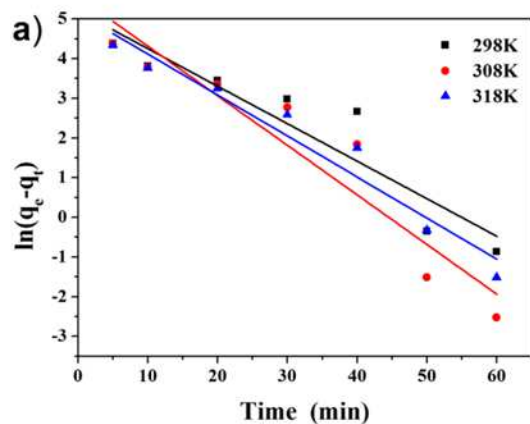


Fig. 10 (a) Pseudo-first-order kinetics; (b) Pseudo-second-order kinetics of uranium(VI) adsorption, $C_0=200\text{mg/L}$, $\text{pH}=5$.

where k_2 ($\text{g}/\text{mg} \cdot \text{min}$) is the rate constant of pseudo-second-order adsorption. As shown on the Fig. 10b and Tab.S 4, the experimental data most closely agree with the pseudo-second-order kinetic models with high correlation coefficients. Therefore, the adsorption kinetic fits the pseudo-second-order model. The pseudo-second-order model assumes that the process may be chemical adsorption.

3.7. Effect of other cation ions

For the purpose of evaluating the selectivity of $\text{Mg}_2\text{CO}_3(\text{OH})_2/\text{CC}$, the experiments of selective adsorption were carried out under the optimum conditions and the corresponding result was illustrated in Fig.S2. The presence of Mg^{2+} reduced slightly the uranium(VI) adsorption capacity. The presence of Na^+ , K^+ and Ca^{2+} did not almost affect the adsorption of uranium(VI) on $\text{Mg}_2\text{CO}_3(\text{OH})_2/\text{CC}$. It is evident that the as-prepared $\text{Mg}_2\text{CO}_3(\text{OH})_2/\text{CC}$ adsorbent may be a promising candidate for selective separation of uranium(VI) from effluents.

3.8. Adsorption mechanism and strategy for enrichment of uranium

The possible adsorption mechanism of the $\text{Mg}_2\text{CO}_3(\text{OH})_2/\text{CC}$ adsorbent was illustrated on Sch.2. Firstly, $[\text{Mg}(\text{HCO}_3)]$

(OH)Mg(OH)₂·H₂O was formed undergo the hydrolysis of Mg₂CO₃(OH)₂ which was confirmed by the FT-IR spectra (Fig.11). The two strong and dominant peaks at 1425, 1485 cm⁻¹ are the characteristic peak of bicarbonate, proving that the existence of [Mg(HCO₃)(OH)Mg(OH)₂·H₂O].⁴⁹ Secondly, the

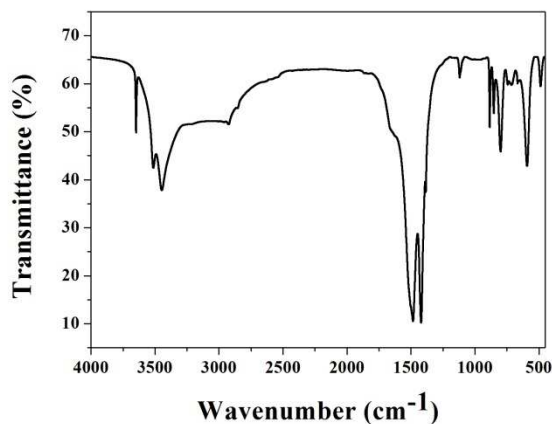
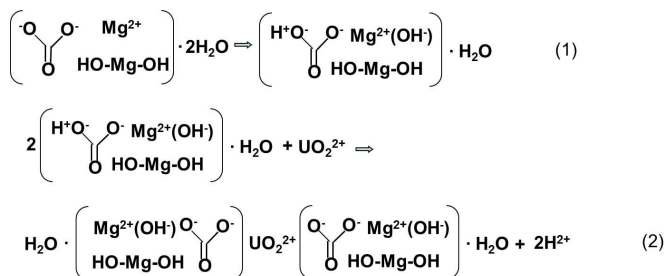


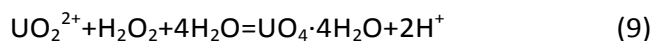
Fig. 11 The FTIR spectrum of as-prepared Mg₂CO₃(OH)₂

uranyl ions replace hydrogen and combine with carbonate ions in aqueous solution.¹⁹ At low pH, the protons of [Mg(HCO₃)(OH)Mg(OH)₂·H₂O] was difficult to substituted with uranyl ions, leading the amount of adsorption reduce. However, high pH was heavily hindered the combination between uranyl and carbonate ions. Therefore, the maximum adsorption capacity at initial pH is 5.0, whereas the final pH of solution is 4.7.



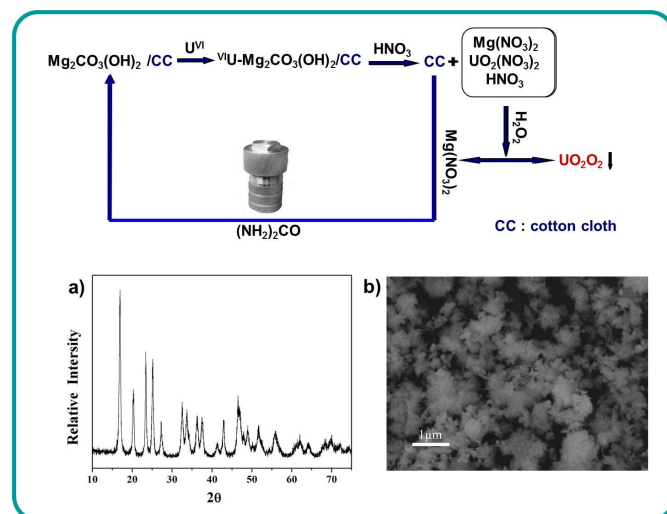
Sch. 2 Supposed mechanism of the adsorption of uranium(VI).

Investigating the process of desorption is important in optimizing the use of adsorbent and improving the economic efficiency. As shown in Sch. 3, a novel strategy was provided for the enrichment of uranyl. First, adsorbent adsorbed uranium was immersed by dilute nitric acid solution to form magnesium nitrate and nitrate ions. Then, to replace the nitrate ions of nitrate ions, excessive amounts of hydrogen peroxide were added to the above solution. A white precipitation of uranyl peroxide was synthesized^{20,50,51} by Eq. (9):



The XRD pattern and SEM image (Sch. 3 a, b) also confirm the formation of uranyl peroxide. Finally, the filtered and worked

supernatant, carboxylated cotton cloth and a certain amount of urea were transferred into Teflon-lined for the regeneration of Mg₂CO₃(OH)₂/CC adsorbent. Moreover, the regenerated Mg₂CO₃(OH)₂/CC adsorbent was sustained excellent adsorption ability after three cycles (Fig.S3), indicating that the as-prepared Mg₂CO₃(OH)₂/CC adsorbent is reusable.



Sch. 3 Design for enrichment of uranyl and recycling of adsorbent,(a),(b) are XRD pattern and SEM image of the UO₂O₂, respectively.

4. Conclusions

The Mg₂CO₃(OH)₂/CC was prepared a facile and cost-effective method for uranium(VI) adsorption. The maximum adsorption capacity of the Mg₂CO₃(OH)₂/CC adsorbent for uranium (VI) was evaluated to be 370 mg/g at 25 °C. Adsorption experiments were conducted by batch technique and the optimum condition for uranium (VI) adsorption is pH value of 5.0, uranium concentration of 200 mg/L and contact time of 60 min. Moreover, the equilibrium data were well consistent with Freundlich isotherms by the pseudo-second-order kinetics. Finally, the adsorption and enrichment of uranium was easy to operate. Such excellent performance may promote the promising and effective adsorbent for practical uranium (VI) adsorption.

Acknowledgements

This work was supported by Heilongjiang Province Natural Science Funds for Distinguished Young Scholar (JC201404), Special Innovation Talents of Harbin Science and Technology for Distinguished Young Scholar (2014RFYXJ005), Fundamental Research Funds of the Central University (HEUCFZ), Natural Science Foundation of Heilongjiang Province (B201316), Program of International S&T Cooperation special project (2013DFR50060), Special Innovation Talents of Harbin Science and Technology (2014RFQXJ087), and the fund for Transformation of Scientific and Technological Achievements of Harbin (2013DB4BG011), Innovation Talents of Harbin Science and

Technology (2014RFQXJ035), Natural Science Foundation of Heilongjiang Province (E201329)

Notes

Supporting Information

Electronic Supplementary Information (ESI) available: details of any supplementary information available should be included here.

Author Information

^a Key Laboratory of Superlight Material and Surface Technology, Ministry of Education, Harbin Engineering University, 150001, PR China.

^b Institute of Advanced Marine Materials, Harbin Engineering University, 150001, PR China.

* Corresponding author: Tel.: +86 451 8253 3026; fax: +86 451 8253 3026; E-mail: zhqw1888@sohu.com.

References

- K. Z. Elwakeel, A. A. Atia and E. Guibal, *Bioresour. Technol.*, 2014, **160**, 107.
- E. Grabias, A. Gladysz-Plaska, A. Ksiazek and M. Majdan, *Environ. Chem. Lett.*, 2014, **12**, 297.
- C. Acharya and S. K. Apte, *Photosynth. Res.*, 2013, **118**, 83.
- H. J. Zhang, H. L. Liang, Q. D. Chen and X. H. Shen, *J. Radioanal. Nucl. Chem.*, 2013, **298**, 1705.
- Z. Chen, Z. Y. Zhuang, Q. Cao, X. H. Pan, X. Guan and Z. Lin, *ACS Appl. Mater. Interfaces.*, 2014, **6**, 1301-1305.
- S. Abbaszadeh, A. R. Keshtkar and M. A. Mousavian, *J. Ind. Eng. Chem.*, 2014, **20**, 1656.
- H. J. Yan, J. W. Bai, X. Chen, J. Wang, H. S. Zhang, Q. Liu, M. L. Zhang and L. H. Liu, *RSC Adv.*, 2013, **3**, 23278.
- U. H. Kaynar, M. Ayvacikli, S. C. Kaynar and U. Hicsonmez, *J. Radioanal. Nucl. Chem.*, 2014, **299**, 1469.
- J. Ramkumar, S. Chandramouleeswaran, B. S. Naidu and V. Sudarsan, *J. Radioanal. Nuc. Chem.*, 2013, **298**, 1845.
- Q. Cao, Y. C. Liu, C. Z. Wang and J. S. Cheng, *J. Hazard. Mater.*, 2013, **263**, 311.
- D. Humelnicu, C. Blegescu and D. Ganju, *J. Radioanal. Nucl. Chem.*, 2014, **299**, 1183.
- A. A. Elabd, W. I. Zidan, M. M. Abo-Aly, E. Bakier and M. S. Attia, *J. Environ. Radioact.*, 2014, **134**, 99.
- S. Zhang, J. Li, T. Wen, J. Xu and X. Wang, *RSC Adv.*, 2013, **3**, 2754.
- S. Zhang, W. Xu, M. Zeng, J. Li, J. Li, J. Xu and X. Wang, *J. Mater. Chem. A.*, 2013, **1**, 11692.
- A. S. Al-Hobaib and A. A. Al-Suhybani, *J. Radioanal. Nucl. Chem.*, 2014, **299**, 560.
- A. Singh, J. G. Catalano, K. U. Ulrich and D. E. Giammar, *Environ. Sci. Technol.*, 2012, **46**, 6596.
- W. C. Song, M. C. Liu, R. Hu, X. L. Tan and J. X. Li, *Chem. Eng. J.*, 2014, **246**, 269.
- J. Kennedy et al., *British Report.*, 1964, **September**, 4516.
- R. V. Davis et al., *Nature.*, 1964, **203**, 1110.
- K. W. Kim, J. T. Hyun, K. Y. Lee, E. H. Lee, K. W. Lee, K. C. Song and J. K. Moon, *J. Hazard. Mater.*, 2011, **193**, 52.
- O. Karnitz, L. V. A. Gurgel, R. P. de Freitas and L. F. Gil, *Carbohydr. Polym.*, 2009, **77**, 646.
- F. V. Pereira, L. V. A. Gurgel and L. F. Gil, *J. Hazard. Mater.*, 2010, **176**, 858.
- L. S. Tan, J. Xu, X. Q. Xue, Z. M. Lou, J. Zhu, S. A. Baig and X. H. Xu, *RSC Adv.*, 2014, **4**, 45924.
- O. Karnitz, L. V. A. Gurgel and L. F. Gil, *Carbohydr. Polym.*, 2010, **79**, 186.
- K. A. G. Gusmao, L. V. A. Gurgel, T. M. S. Melo and L. F. Gil, *J. Environ. Manage.*, 2013, **118**, 138.
- J. Huang, M. Ye, Y. Q. Qu, L. F. Chu, R. Chen, Q. Z. He and D. F. Xu, *J. Colloid Interface Sci.*, 2012, **385**, 141.
- S. F. Li, Y. M. Shen, D. B. Liu, L. H. Fan, X. C. Zheng and J. Yang, *Compos. Interfaces.*, 2012, **19**, 493.
- T. Ohkubo, S. Suzuki, K. Mitsuhashi, T. Ogura, S. Iwanaga, H. Sakai, M. Koishi and M. Abe, *Langmuir.*, 2007, **23**, 5873.
- N. Singh and K. Balasubramanian, *RSC Adv.*, 2014, **4**, 27694.
- Z. B. Zhang, Z. W. Zhou, X. H. Cao, Y. H. Liu, G. X. Xiong and P. Liang, *J. Radioanal. Nucl. Chem.*, 2014, **299**, 1483.
- S. A. Sadeek, M. A. El-Sayed, M. M. Amine and M. O. Abd El-Magied, *J. Radioanal. Nucl. Chem.*, 2014, **299**, 1303.
- S. Kerisit and C. X. Liu, *Environ. Sci. Technol.*, 2014, **48**, 3903.
- H. S. Zhang, J. Wang, B. Zhang, Q. Liu, S. N. Li, H. J. Yan and L. H. Liu, *Colloids Surf. A.*, 2014, **444**, 134.
- H. N. Bhatti and S. Hamid, *International J. Environ. Sci. Technol.*, 2014, **11**, 818.
- C. Cheng, Z. Y. Liu, X. X. Li, B. H. Su, T. Zhou and C. S. Zhao, *RSC Adv.*, 2014, **4**, 42352.
- I. C. Popescu, P. Filip, D. Humelnicu, I. Humelnicu, T. B. Scott and R. A. Crane, *J. Nucl. Mater.*, 2013, **443**, 253.
- X. K. OuYang, R. N. Jin, L. P. Yang, Y. G. Wang and L. Y. Yang, *RSC Adv.*, 2014, **4**, 28703.
- X. Yu, S. Tong, M. Ge, J. Zuo, C. Cao and W. Song, *J. Mater. Chem. A.*, 2013, **1**, 960.
- S. H. Ahmed, E. M. El Sheikh and A. M. A. Morsy, *J. Environ. Radioact.*, 2014, **134**, 125.
- P. Rule, K. Balasubramanian and R. R. Gonte, *J. Environ. Radioact.*, 2014, **136**, 26.
- G. K. Incili and G. A. Aycik, *J. Radioanal. Nucl. Chem.*, 2014, **301**, 423.
- G. W. Peng, D. X. Ding, F. Z. Xiao, X. L. Wang, N. Hun, Y. D. Wang, Y. M. Dai and Z. Cao, *J. Radioanal. Nucl. Chem.*, 2014, **301**, 785.
- B. Ivanova and M. Spittler, *J. Environ. Radioact.*, 2014, **135**, 80.
- D. P. Dutta, A. Mathur, J. Ramkumar and A. K. Tyagi, *RSC Adv.*, 2014, **4**, 37033.
- X. L. Yu, D. J. Kang, Y. Y. Hu, S. R. Tong, M. F. Ge, C. Y. Cao and W. G. Song, *RSC Adv.*, 2014, **4**, 31367.
- S. Zhang, X. W. Shu, Y. Zhou, L. Huang and D. B. Hua, *Chem. Eng. J.*, 2014, **253**, 59.
- S. Sen Gupta and K. G. Bhattacharyya, *RSC Adv.*, 2014, **4**, 28577.
- S. Zhang, M. Zeng, J. Li, J. Li, J. Xu and X. Wang, *J. Mater. Chem. A.*, 2014, **2**, 4394.
- Choudhari, B. P. et al., *Indian. J. Chem.*, 1972, **10**, 28265.
- K. A. H. Kutatko, K. B. Helean, A. N. Navrotsky, P. C. Burns, *Science.*, 2003, **302**, 1191.
- R. Gupta, V. M. Pandey, S. R. Praneesh, A. B. Chakravarty, *Hydromet.*, 2004, **71**, 432.